Supplementary Information

Co-binding of pharmaceutical compounds at mineral surfaces: Molecular investigations of dimer formation at goethite/water interfaces

Jing Xu [a,b], Rémi Marsac [b#], Dominique Costa [c], Wei Cheng[b], Feng Wu [d], Jean-François Boily [e], Khalil Hanna [b]*

[a]State Key Laboratory of Water Resources and Hydropower Engineering Science, Wuhan University, Wuhan 430072, China

[b]Ecole Nationale Supérieure de Chimie de Rennes, CNRS, UMR 6226, 11 Allée de Beaulieu, CS 50837, 35708 Rennes Cedex 7, France.

[c]Institut de Recherches de Chimie de Paris UMR 8247 ENSCP Chimie Paristech, 11 rue P. Et M. Curie, 75005 Paris, France.

[d]Hubei Key Lab of Biomass Resource Chemistry and Environmental Biotechnology, School of Resources and Environmental Science, Wuhan University, Wuhan, 430079, P. R. China

[e]Department of Chemistry, Umeå University, Umeå, SE-901 87, Sweden

*Corresponding author: Tel.: +33 2 23 23 80 27, khalil.hanna@ensc-rennes.fr

[#]Present address: Géosciences Rennes, UMR CNRS 6118, Université de Rennes 1, Campus de Beaulieu, CS74205, 35042 Rennes Cedex, France

A manuscript re-submitted to *ES&T*

June, 2017

(26 pages, 16 figures, 2 tables)

I. Synthesis and characterization of goethite

Goethite (α-FeOOH) was prepared following Mazeina and Navrotsky's work[1]. Briefly, 500 mL 2.5 M KOH was added to 120 ml 0.5 M $Fe(NO_3)_3 \cdot 9H_2O$ solution at a rate of 4 mL/min with stirring in Nalgene bottle. Nitrogen was purged before and during the synthesis procedure in order to remove dissolved carbon dioxide. The mixture was then aged for 98h at 60 ^oC. After precipitation, the solid were dialyzed for 2 weeks using Spectra/Por® Dialysis Tubing (MWCO: 1kD), water was change every day until water conductivity was < 5 μS/cm. The resulting goethite was stored as aqueous suspensions in a Nalgene bottle at ambient temperature in the dark. Gibbsite ($Al(OH)_3$) was synthesized as described elsewhere.[2] To verify the nature of minerals, solid samples were analyzed by X-ray powder diffraction (XRD) using a D8 Bruker diffractometer, equipped with a monochromator and a position-sensitive detector. The X-ray source was a Co anode (λ = 0.179 nm). Acicular particles of 100-200 nm / 30-50 nm were obtained using Transmission electron microscopy JEM-2100 (JEOL). The Brunauer-Emmett-Teller (BET) specific surface area (81 m^2/g) and isoelectric point (9.1) were also determined.

II. Sorption data under ambient atmosphere versus $N_{2(g)}$ bubbling

pH-edges were recorded under ambient atmosphere or under $N_{2(g)}$ bubbling to investigate the effect of dissolved CO_2 on the sorption of NA ($[NA]_{tot}$ = 20 μM) and NFA ($[NFA]_{tot}$ = 20 μM) in single and binary system. Results in Fig. S1 showed that dissolved CO_2 has only a significant effect on NA and NFA sorption to goethite for pH > 6.5.

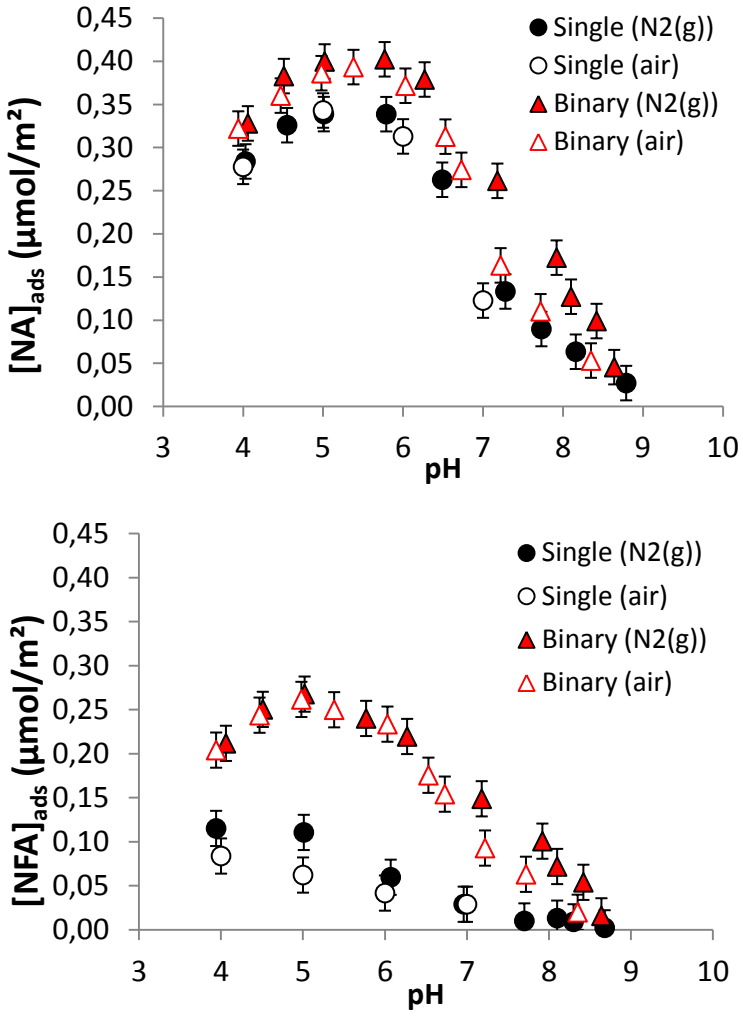

Figure S1. Experimental effects of pH and dissolved CO_2 (i.e. ambient air or $N_{2(g)}$ bubbling) on (a) NA single ($[NA]_{tot}$ = 20 µM) and binary ($[NA]_{tot}$ = $[NFA]_{tot}$ = 20 µM) and (b) NFA single ($[NFA]_{tot}$ = 20 µM) and binary ($[NFA]_{tot}$ = $[NA]_{tot}$ = 20 µM) systems at ionic strength 10 mM (NaCl).

III. Solubility test for NA and NFA

NA and NFA solubility experiments (undersaturation direction) were conducted following the procedure used for oxolinic acid.[3] Solid NA or NFA (~3-5 mg) were suspended in 10 mL of solution in 10 mM NaCl as a function of pH. The suspensions were equilibrated for 24 h, after which the supernatants were filtered (0.2 µm) and NA or NFA concentrations were measured with HPLC.

NA and NFA aqueous concentrations are plotted versus pH on the figure below. NA solubility is low and constant with pH for pH < 6 ($[NA]_{aq}$ = 80 µM). This result is in agreement with the range of literature solubility data at pH = 5: $[NA]_{aq}$ = 83-128 µM at pH 5.[4] NA solubility increases by one order of magnitude for each increase of 1 pH unit for pH > 7.

NA speciation and solubility can be described with the following equations:

$NAH_{(aq)} \rightleftharpoons NA^-_{(aq)} + H^+_{(aq)}$; $K_{a,NA}$

$NAH_{(s)} \rightleftharpoons NAH_{(aq)}$; $K_{s,NA}$

Where $K_{a,NA}$ and $K_{s,NA}$ are the acidity and the solubility constants of NA, respectively. By using $pK_{a,NA}$ = 6.10 (calculated at an ionic strength (I) of 0.01 M using the data of Ross and Riley[4] for I = 0.15 M the Davies equation) and $K_{s,NA}$ = 80 µM, NA solubility can be predicted (See the figure below).

NFA solubility is similar to NA for 3 < pH < 4.5 ($[NFA]_{aq}$ = 78 µM). This value agrees with literature data: $[NFA]_{aq}$ = 76 µM.[5] NFA solubility increases with (i) decreasing pH for pH < 3 and (ii) increasing pH for pH > 4.5.

NFA speciation and solubility can be described with the following equations:

$NFAH_2^+{}_{(aq)} \rightleftharpoons NFAH_{(aq)} + H^+_{(aq)}$; $K_{a1,NFA}$

$NFAH_{(aq)} \rightleftharpoons NFA^-_{(aq)} + H^+_{(aq)}$; $K_{a2,NFA}$

$NFAH_{(s)} \rightleftharpoons NFAH_{(aq)}$; $K_{s,NFA}$

Where $K_{a1,NFA}$, $K_{a2,NFA}$ and $K_{s,NFA}$ are the two acidity and the solubility constants of NA, respectively. By using $pK_{a1,NFA}$ = 2.28, $pK_{a2,NFA}$ = 5.01 (calculated for I = 0.01 M using the data of Takacs-Novak and Tam for I = 0.15 M the Davies equation)[6] and $K_{s,NFA}$ = 78 µM, NFA solubility can be predicted (See Fig. S2).

To test whether NA and NFA can interact in solution, both NA and NFA solids (~3-5 mg each) were suspended in the same solution, and solubility of NA and NFA was investigated following the same procedure. The figure below shows that no solubility data coincide with single systems, i.e. no solubility enhancement is observed, which would have traduced the formation of NA-NFA aqueous complexes.

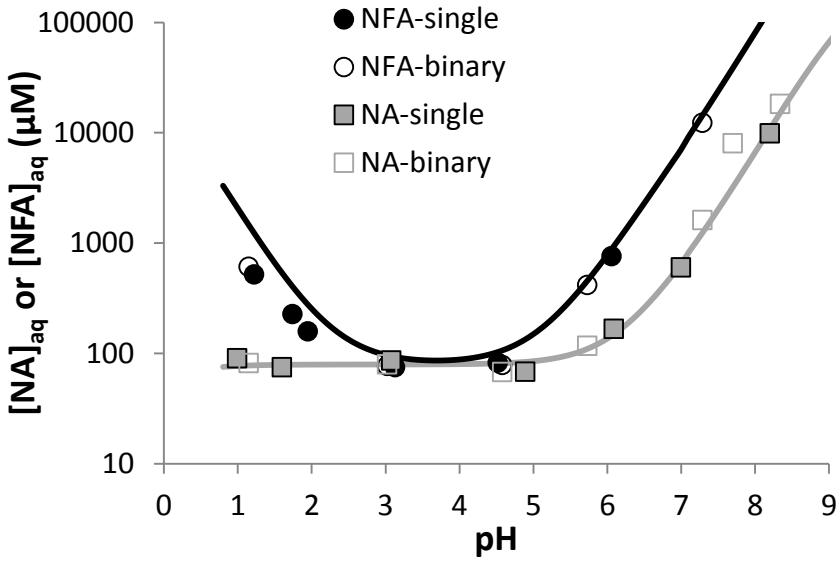

Figure S2. Solubility of NA and NFA in single and binary system as a function of pH in 10 mM NaCl solutions.

IV. Desorption tests

According to the preliminary test, adsorption of these three components was negligible at pH = 11. Therefore, desorption test was conducted by adjusting pH higher than 11 after the system reached equilibrium, and then stirred for around 2 h. As can be seen from Table S1, an average recovery of 99±2% for the investigated drugs was obtained.

Table S1. Desorption data (%) of each component in various systems

System	Components	pH

		4	5	6	7
Single	NA	100.1	98.7	98.0	100.9
	NFA	102.4	105.7	97.9	98.2
	SMX	99.5	98.7	97.5	99.4
binary	NA (with NFA)	100.7	97.0	100.3	95.9
	NA (with SMX)	107.2	99.3	96.5	105.9
	NFA (with NA)	97.7	96.6	98.7	96.4
	NFA (with SMX)	98.5	99.6	100.9	101.2
	SMX (with NA)	100.6	100.7	101.2	101.8
	SMX (with NFA)	100.3	98.7	101.3	97.5

***** The reproducibility of the measurements was around 5% for each component.

V. Kinetic and batch sorption in single and binary system

Kinetic adsorption experiments of NA and NFA in single ($[NA]_{tot}$ = 20 μM; $[NFA]_{tot}$ = 20 μM) and binary ($[NA]_{tot}$ = $[NFA]_{tot}$ = 20 μM) systems were conducted at pH 6 in 10 mM NaCl for 0.5 g/L of goethite under ambient atmosphere. Desorption tests showed that NA and NFA were removed only by adsorption, and that oxidation of sorbed molecules did not occur under our experimental conditions (Table S1). The adsorption kinetics results are shown on Fig. S3. Batch kinetic experiments showed the adsorption of NA and NFA onto goethite at pH 6 increased quickly in the first hour of contact time, and then slowly in a second stage before achieving equilibrium after 6 h (Fig. S3).

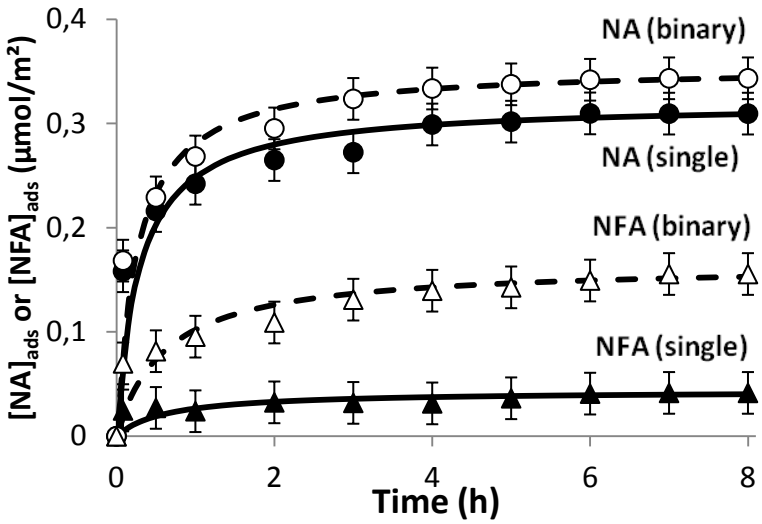

Figure S3. Adsorption kinetics of NA and NFA on 0.5 g/L goethite in single ($[NA]_{tot}$ = 20 µM or $[NFA]_{tot}$ = 20 µM) and binary ($[NA]_{tot}$ = $[NFA]_{tot}$ = 20 µM) systems at pH 6 and ionic strength 10 mM (NaCl). Lines show the best fit with a pseudo-second-order kinetic model.

A pseudo-second-order model was used to fit the kinetic data, which can be express as:

$$\frac{dq}{dt} = k_2(q_e - q_t)^2 \quad \text{(S1)}$$

Where k_2 (m^2/µmol·min) is the pseudo-second-order rate constant, q_e and q_t is the amount of adsorbed NA or NFA at equilibrium and at time t, respectively. Integration of eq. S1 gives: $\frac{t}{q_t} = \frac{1}{k_2 q_e^2} + \frac{1}{q_e}t$ (S2)

k_2 and q_e were calculated from the slope and y-intercept of the plots of t/q_t vs. t. The obtained constants are shown in Table S2.

Table S2. Kinetic data of NA and NFA fitting to pseudo-second-order model

	q_e (μmol/m^2)	k_2 (m^2/μmol·min)	r^2
NA single	0.32	0.18	0.998
NFA single	0.04	0.60	0.975
NA binary	0.35	0.18	0.999
NFA binary	0.16	0.16	0.992

The kinetic behavior is quite similar in both single and binary systems, except that the amounts of NA or NFA adsorbed to goethite in the NA/NFA binary system are larger than for the corresponding single system. This greater adsorption is observed in the NA/NFA equimolar mixture could be due to the cooperative adsorption occurred between NA and NFA. In contrast to NA (where $k_{NA,single}$ = 0.180 m^2/μmol·min (R^2 = 0.998) ≈ $k_{NA,binary}$ = 0.178 m^2/μmol·min (R^2 = 0.999)), the kinetic rate constant of NFA in binary systems (0.16 m^2/μmol·min, R^2 = 0.992) is almost 4 times less compared to the corresponding single system (0.60 m^2/μmol·min, R^2 = 0.975), suggesting modification of adsorption mechanism of NFA in binary systems.

The adsorption kinetics were also conducted with SMX (Fig. S4). No cooperative effect was observed in the equimolar mixture neither with NA nor NFA (Fig. S4a). The adsorption of SMX onto goethite in the single system is insignificant, and does not change in the presence of NFA or NA (Fig. S4b). The lack of SMX binding to goethite surfaces is likely due to the absence of carboxyl and carbonyl functional groups in

SMX molecule (see below), groups that are supposed to ensure hydrogen bonds with surface hydroxo groups of mineral.

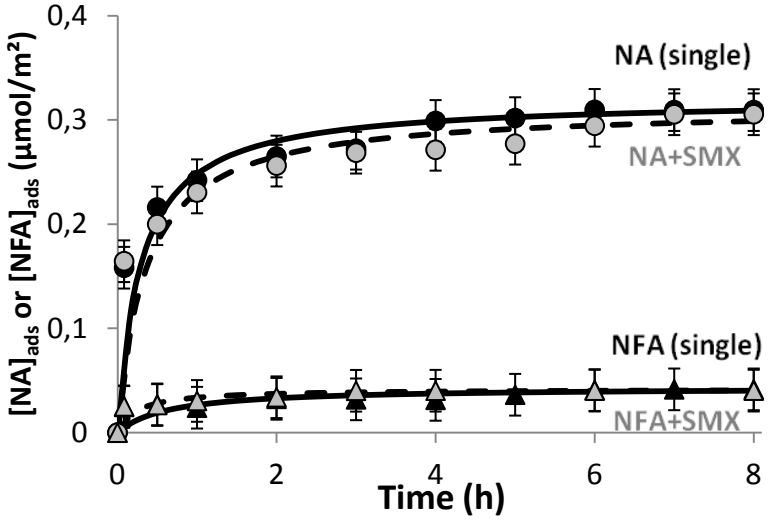

Figure S4a. Adsorption kinetics of NA ($[NA]_{tot}$ = 20 µM, circle) and NFA ($[NA]_{tot}$ = 20 µM, triangle) on 0.5 g/L goethite in single and binary systems with SMX ($[SMX]_{tot}$ = 20 µM) at pH = 6 and ionic strength 10 mM (NaCl). Lines show the best fit with a pseudo-second-order kinetic model.

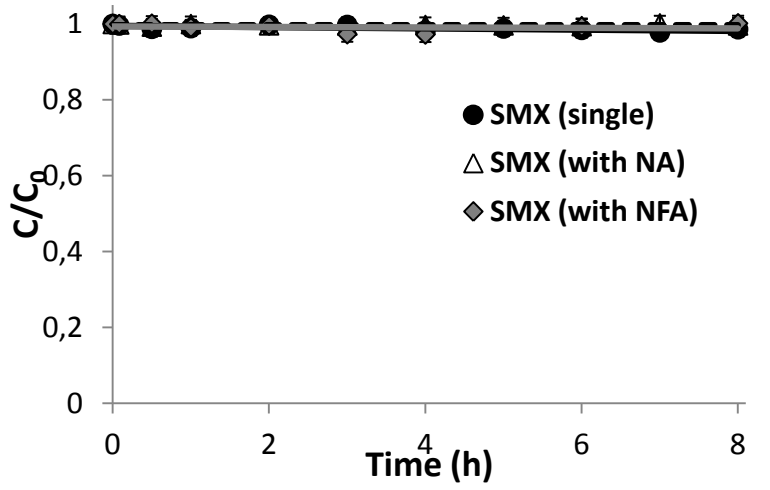

Figure S4b. Adsorption kinetics of SMX ($[SMX]_{tot}$ = 20 µM) alone, with NA (20 µM or NFA (20 µM) on 0.5 g/L goethite in single and binary systems at pH = 6 in 10 mM NaCl.

VI. Species distribution of NA, NFA and SMX

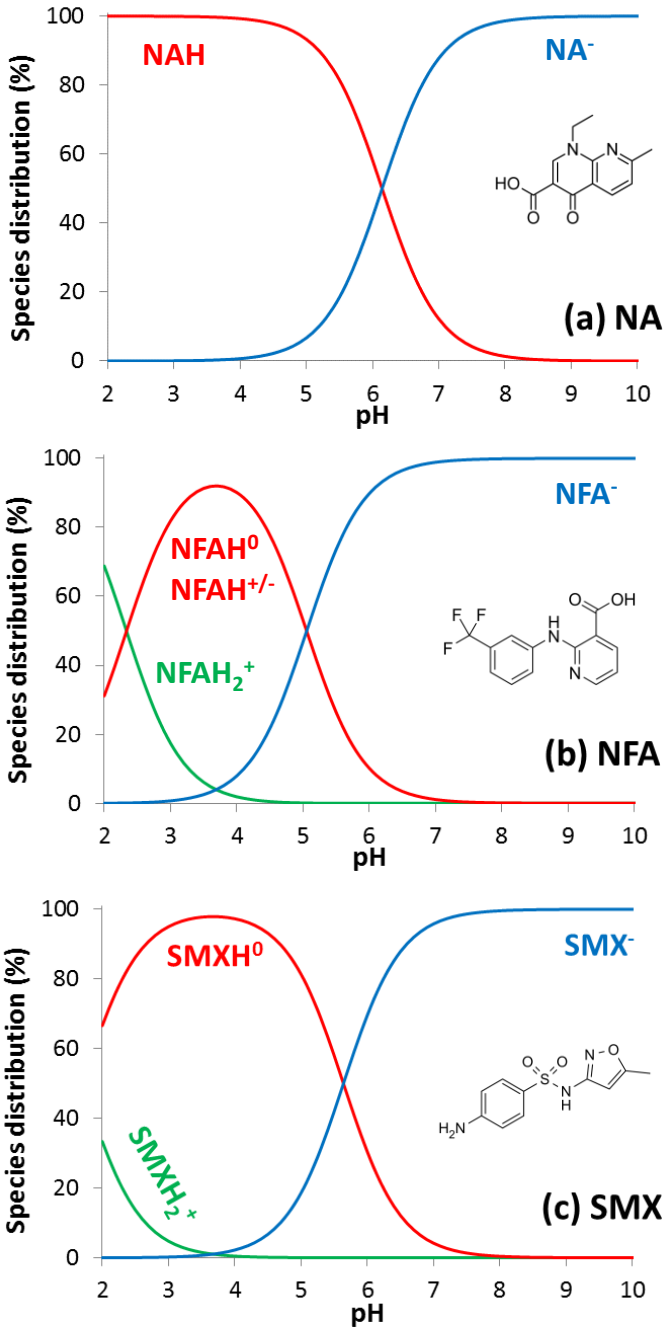

Figure S5. Distribution of (a) NA, (b) NFA, (c) SMX at various pH values. Ionic strength: 10 mM NaCl. The neutral form of molecules is shown on the right side.

VII. ATR-FTIR investigations

Single systems. The ATR-FTIR spectra of solid $NA_{(s)}$ and $NFA_{(s)}$ and soluble $NA_{(aq)}$ and $NFA_{(aq)}$ were used as a basis for assigning surface-bound NA species. Owing to the low solubility of NA and NFA, band assignments in the soluble species were made from a 1 M NaOH solution. The solid form of NA and NFA was analyzed using ATR-FTIR by loading powder on the crystal and then a drop of water was added to apply it more uniformly. The effect of pH (4-6) on NA and NFA sorption to goethite in 10 mM NaCl was investigated for $[NA]_{tot}$ or $[NFA]_{tot}$=100 µM. Results for NA and NFA are shown in Fig. S6a and S6b, respectively. The bands at 1706 cm^{-1} and 1660 cm^{-1} that were found in $NA_{(s)}$ and $NFA_{(s)}$, respectively, correspond to the C=O stretching mode of the protonated carboxylic group.[7] These bands disappear in solution and at the goethite surface while two other bands appear, corresponding to $\nu_{COO,as}$ ($NA_{(aq)}$: 1578 cm^{-1}; $NFA_{(aq)}$: 1517 cm^{-1}) and $\nu_{COO,s}$ ($NA_{(aq)}$: 1392 cm^{-1}; $NFA_{(aq)}$: 1386 cm^{-1}). No significant effect of pH on adsorbed NA or NFA is observed for $4 < pH < 6$.

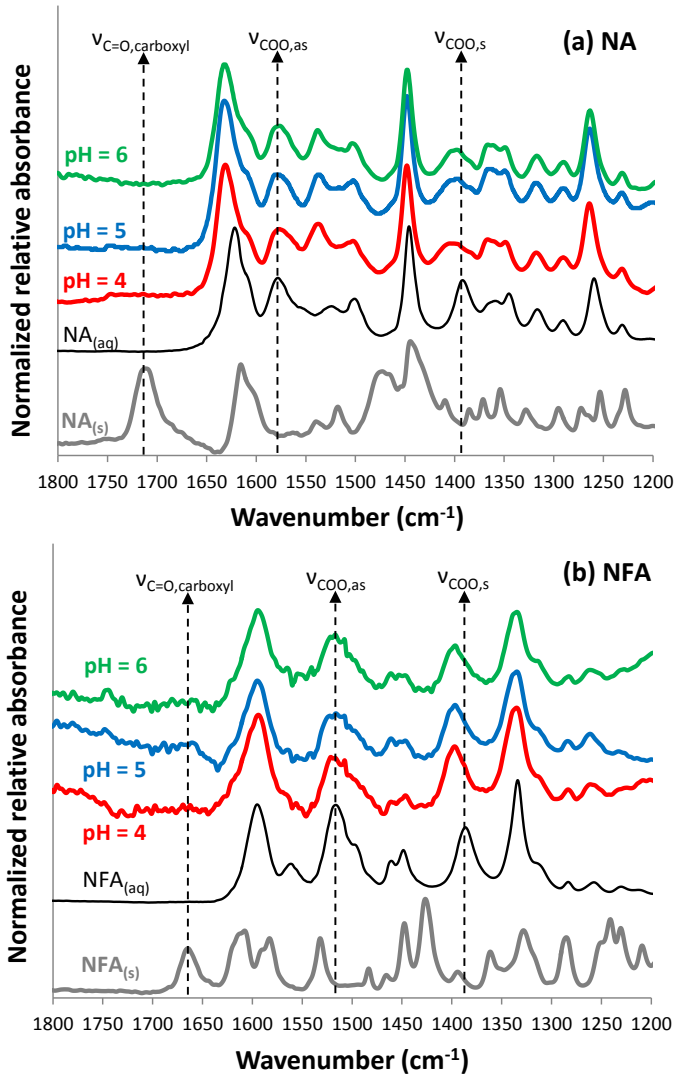

Figure S6. ATR-FTIR spectra at different pH values. (a) Comparison between $NA_{(aq)}$ (in 1M NaOH), $NA_{(s)}$ and goethite-NA at pH = 4, 5 and 6. (b) Comparison between $NFA_{(aq)}$ (in 1M NaOH), $NFA_{(s)}$ and goethite-NFA at pH = 4, 5 and 6.

Binary systems. In the main text, the ATR-FTIR spectra recorded for constant $[NA]_{tot}$ (100 µM) and increasing $[NFA]_{tot}$ (0, 10, 20, 50 and 100 µM) at pH = 6, [NaCl] = 10 mM and 0.5 g/L of goethite are presented. The contribution of NFA to these spectra is tentatively suppressed by subtracting the goethite-NFA spectrum to the various goethite-NA-NFA spectra. The corrected spectra, normalized to the band at 1448 cm^{-1}, are compared with the spectra of goethite-NA and $NA_{(aq)}$ (Fig. S7a). As stated in the

main text, corrected spectra do not correspond to the goethite-NA one, which further highlighted the spectral modifications upon co-binding of NA/NFA at goethite surfaces. Major spectral variation are found for a peak maximum found at 1522 cm^{-1}, which might correspond to a red-shift of $\nu_{C=C,ring}$(NA) upon NA-NFA interaction at goethite surfaces, and a drastic increase of a band at 1350 cm^{-1}, which suggests the perturbation of C-C stretching and/or C-H bending in the aromatic and pyridine rings of NFA (i.e. a splitting of $\nu_{1,ring}$(NFA)) upon interaction with NA at goethite surface.

Fig. S7b shows ATR-FTIR spectra at constant $[NFA]_{tot}$ (100 µM) and increasing $[NA]_{tot}$ (0, 10, 20, 50 and 100 µM).

Finally, Figure S8 shows similar experiments than in Fig. 4 (main text) but for lower loadings ($[NA]_{tot}$ = 20 µM; 10 < $[NFA]_{tot}$< 40 µM). Although the signal to noise ratio is much lower, the same conclusions can be drawn up.

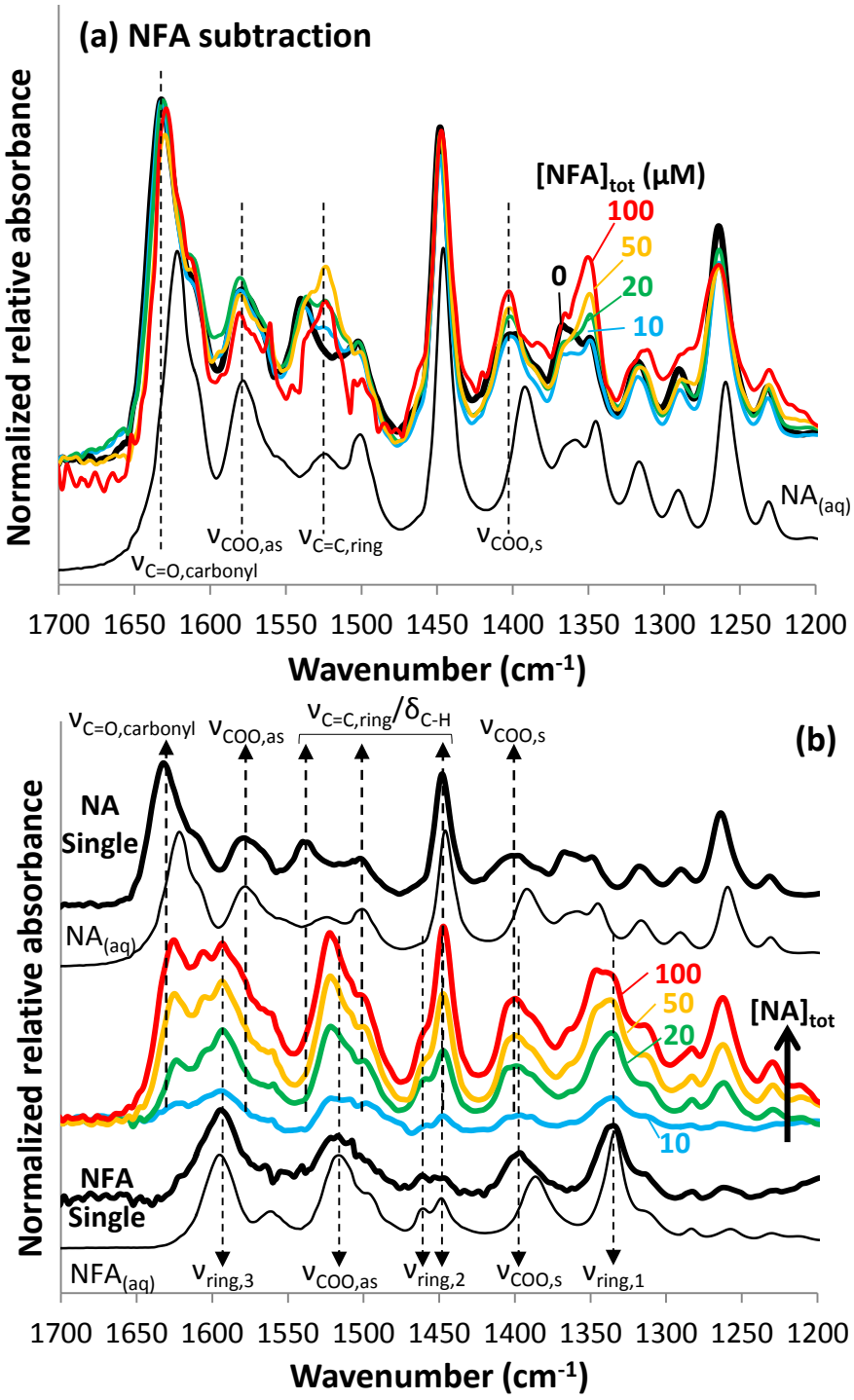

Figure S7. ATR-FTIR spectroscopy. (a) Subtraction of goethite-NFA spectrum to the 100 µM $[NA]_{tot}$ with varying $[NFA]_{tot}$ spectra (see Fig. 4 in the main text). The spectrum of dissolved NA in 1 M NaOH is shown for comparison. (b) From top to bottom: NA single system ($[NFA]_{tot}$ = 100 µM), dissolved NA ($NA_{(aq)}$ in 1 M NaOH), NA-NFA binary system ($[NFA]_{tot}$ = 100 µM, 10 < $[NA]_{tot}$< 100 µM; the arrows show increasing $[NA]_{tot}$), NFA single system ($[NFA]_{tot}$ = 100 µM), dissolved NFA ($NFA_{(aq)}$ in 1 M NaOH).

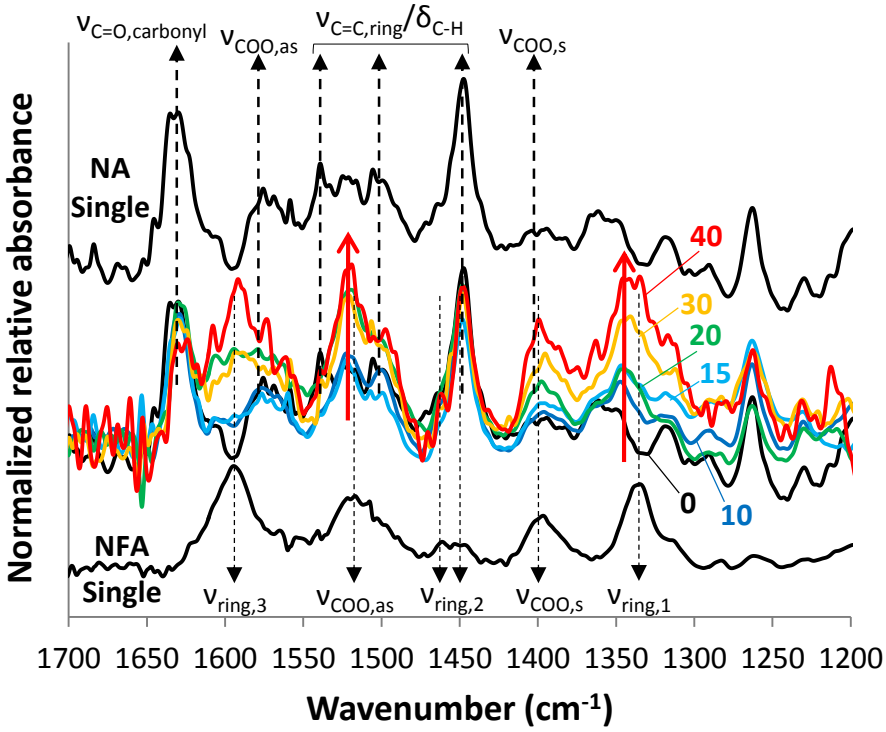

Figure S8. ATR-FTIR spectroscopy. From top to bottom: NA single system ($[NA]_{tot}$ = 20 µM), NA-NFA binary system ($[NA]_{tot}$ = 20 µM, 10 < $[NFA]_{tot}$< 40 µM), NFA single system ($[NFA]_{tot}$ = 100 µM).

ATR-FTIR investigations of binding mechanisms

ATR-FTIR spectra of unbound compound ($NA_{(aq)}$ or $NFA_{(aq)}$) and goethite bound compound at pH = 6 are shown in Fig. S6. The absence of the band at 1706 cm^{-1} that is otherwise manifested in $NA_{(s)}$ powder (see Fig. S6 for bands assignments) is attributed to the C=O stretching mode of the protonated carboxylic group. This suggests that NA sorbs to goethite in its unprotonated form.[7] The symmetric stretching band of the carboxylate ($\nu_{COO,s}$) at 1392 cm^{-1} of $NA_{(aq)}$ is broader on goethite, which is taken as an indication of interactions of carboxylic groups with surface hydroxo groups with various hydrogen-bond strengths (cf. inhomogeneous band broadening[8]). In addition,

the intensity of the 1365 cm^{-1} band of the bound NA is larger than that of 1340 cm^{-1} when at goethite surfaces, a result that could be attributed to a shift of $\nu_{COO,s}$ upon the formation of a metal bonded (MB) complex.[3] By contrast, the asymmetric stretching band of the carboxylate ($\nu_{COO,as}$) at 1578 cm^{-1} is not affected by adsorption. The difference between $\nu_{COO,as}$ and $\nu_{COO,s}$ is larger for MB complex than for $NA_{(aq)}$ suggesting that one oxygen of the carboxylate binds to one surface Fe.[9] The band at 1540 cm^{-1} for NA on goethite can be attributed to a blue-shift of C=C stretches ($\nu_{C=C,ring}$) in the quinolinone ring due to variations of the electronic distribution in NA molecule upon surface complexation.[10] A blue shift of $\nu_{C=O,carbonyl}$ (1642 cm^{-1}) compared to $NA_{(aq)}$ suggests the involvement of the keto group in the surface complex, in addition to one oxygen of the carboxylate. A similar conclusion was also proposed in some previous work.[3,11,12] However, we cannot directly conclude from the ATR-FTIR spectra alone whether this complex involves one or more surface Fe.

As for NA, the absence of the band corresponding to the C=O stretching mode of NFA protonated carboxylic group (~1660 cm^{-1}, as assigned in $NFA_{(s)}$ spectrum; see Fig. S7) suggests that it also sorbs to goethite in its unprotonated from. The asymmetric stretching band of the carboxylate ($\nu_{COO,as}$) (1517 cm^{-1}) is not affected by adsorption whereas the $\nu_{COO,s}$ (1386 cm^{-1} for $NFA_{(aq)}$) band is slightly blue-shifted (1392 cm^{-1}) and broader on goethite. These observations are consistent with previous ones made for monocarboxylate ligands, e.g., acetate or benzoate[13] and suggest the formation of HB or OS complexes. Other bands (denoted $\nu_{1,ring}$ to $\nu_{4,ring}$) correspond mainly to C-C stretching and/or C-H bending in the aromatic and pyridine rings.[14,15]

ATR-FTIR spectra of bound NFA or NA recorded at different pH values (from 4 to 6) showed no significant modification in the main absorption bands of sorbed compounds (Fig S6).

VIII. DFT study

The adsorption was studied on gibbsite $AlOH_3$ and diaspore AlOOH. Figure S9 shows the model of gibbsite and diaspore.

The bulk gibbsite was optimized, and the optimized cell parameters are 8.53, 4.98 and 9.55 Å, b = 94.5) to be compared to the experimental ones, a = 8.68 Å, b = 5.08 Å, c = 9.74 Å and β = 94.54.[16] To model the non-site specific adsorption observed in the present study, we choose to use the basal surfaces. The basal plane (001) was chosen. The surface is composed of Al_{VI} fold coordinated and 2-OH groups. The pKa of the basal plane OH groups is 5.9.[17] To model the surface, a two layers slab was cut and the first sheet was let free to relax, with the cell parameters constrained to that of the bulk. A (2x2) cell was built to obtain a large cell enough to allow adsorption of the molecules without significant interactions between the molecules.

Following the same procedure, the bulk diaspore was optimized. The cell parameters are 4.39 9.40 and 2.84 for a = 4.4007 Å, b = 9.4253 Å, c = 2.8452 Å experimentally.[18] A (010) surface was built. Water molecules were adsorbed on the Al5c surface atoms, as performed by Kubicki et al[19] in the case of goethite. Notice that several surface terminations may exist, $AlOH_2$, AlOH and AlO_3. Here we choose to build the «associative water adsorbed» model, consisting in molecular water adsorbed

on Al ions. A (4x4) cell was chosen to build the diaspore surface.

A)	B)
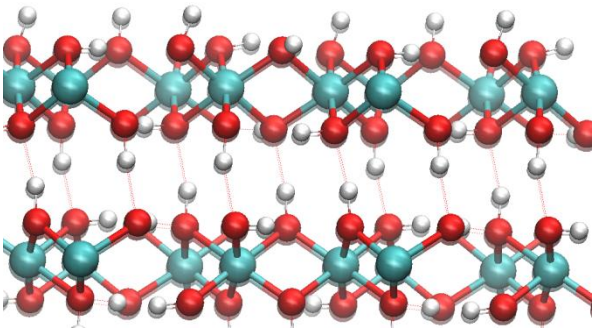	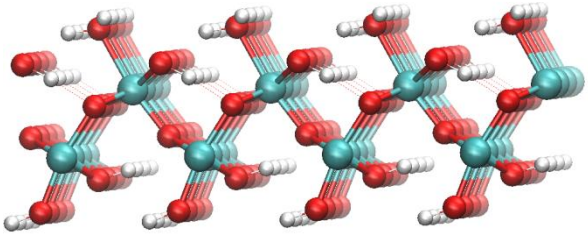
Figure S9. A) Gibbsite basal surface B) diaspore basal surface covered with one water monolayer	

Energetics. The adsorption energies were calculated as:

Adsorption of NA or of NFA on the surface:

Eads(NA) = E(surface-NA) - E(NA) - E(surface),

Eads(NFA) = E(surface-NFA) - E(NFA) - E(surface),

Adsorption of the NA-NFA dimer,

Eads(dimer) = E(surface-dimer) - E(dimer) -E(surface),

Where E(dimer) is the energy of the optimized NA-NFA dimer in gas phase,

Energy of adsorption of the dimer decomposed into each separate consituant,

Eads(mol) = E(surface-dimer) - E(NA) - E(NFA) -E(surface),

Adsorption of NFA on preadsorbed NA,

Eads(NFA/NA) = E(surface-dimer) - E(surface-NA) - E(NFA) -E(surface)

And for the dimer formation, E(dimer-formation) = E(dimer) - E(NA) -E(NFA)

Molecules and dimer. Fig. S10 shows the optimized dimer formed for the neutral species. The planes of the two molecules are distant by around 4 Å, compatible with weak interactions. When the NFA anion or cation are considered, the energy of interaction in the dimer is the same, because the protons of the carboxylate or the NH function do not participate to the interaction.

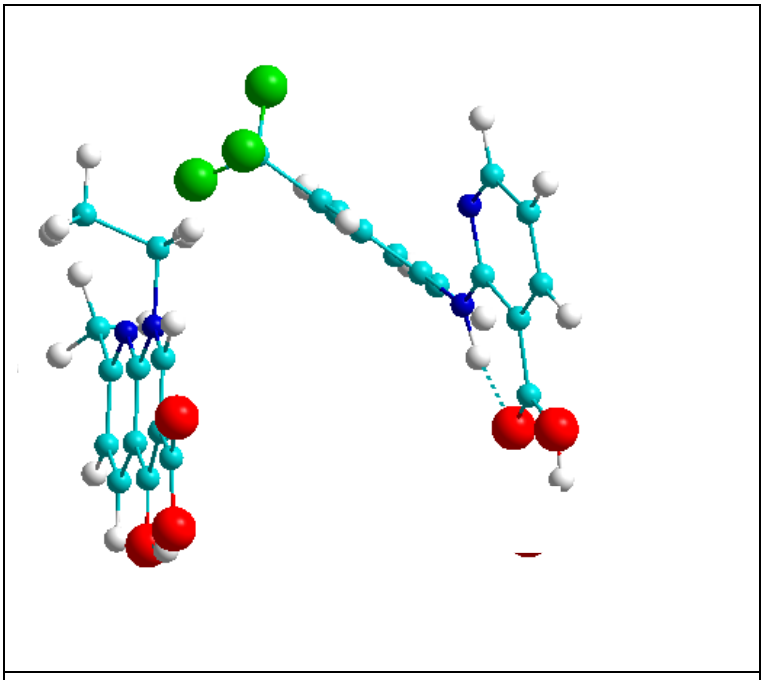

Figure S10. Dimer NA NFA, in the neutral form

Adsorption on gibbsite. Fig. S11 shows the adsorbed NA molecule on gibbsite surface. The inner sphere adsorption considers an anion exchange with the release of a water molecule. The adsorption is endothermic, in the inner sphere mode, and exothermic by 0.23 eV in the outer sphere mode when the molecule is perpendicular to the surface. When the molecule is bent to the surface, it is more exothermic, Eads(NA) = -0.78 eV.

A)	B)	C)
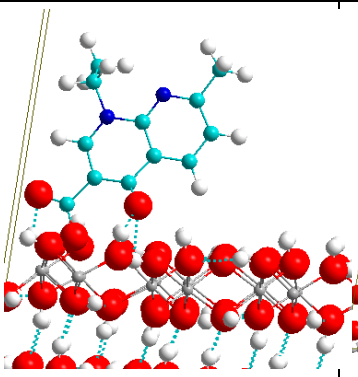	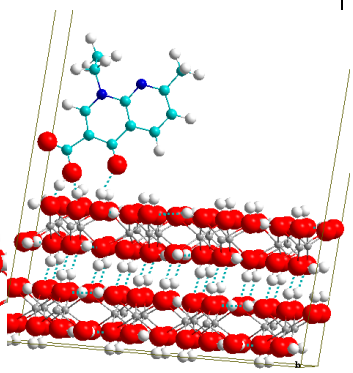	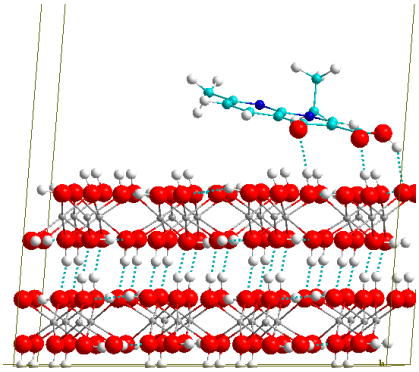
Eads (NA)= 0.86 eV	Eads(NA) = -0.23 eV	Eads(NA) = -0.78 eV

Figure S11. Adsorption geometry and energy of NA on gibbsite in A) the inner, and B) the outer sphere adsorption mode with the molecule perpendicular to the surface, C) outer sphere adsorption with the molecule bent towards the surface

Fig. S12 shows the adsorbed NFA molecule on gibbsite surface. Physisorption of NFA is also favoured at the gibbsite surface, with an energy of adsorption of -0.78 eV.

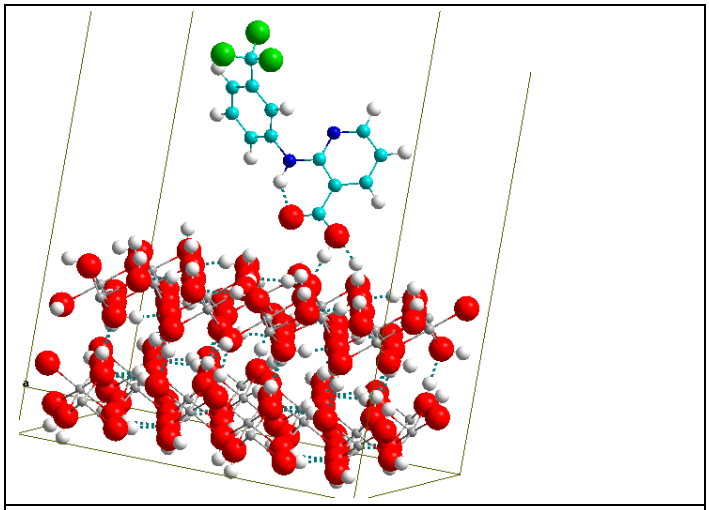

Figure S12. NFA physisorption on the gibbsite surface, Eads(NFA) = -0.78 eV

Fig. S13 shows NA and NFA molecules co-adsorbed on the gibbsite basal surface, with NA adsorbed as inner sphere and outer sphere complexes.

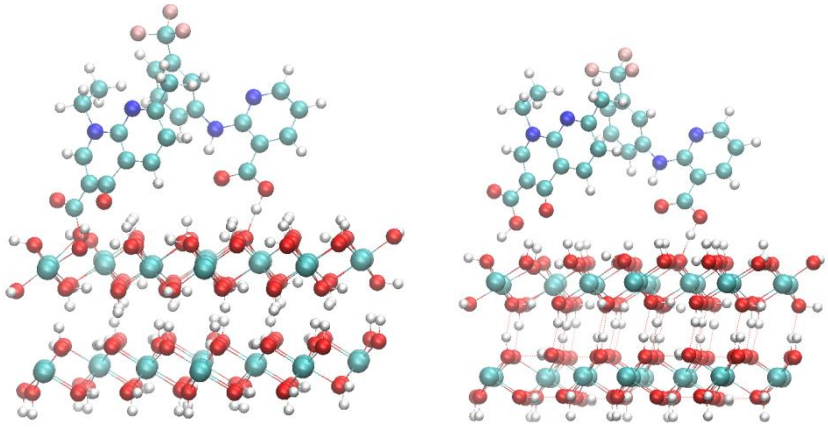

Figure S13. NA and NFA molecules co-adsorbed on the gibbsite basal surface, with NA adsorbed as (*left*) inner sphere and (*right*) outer sphere complexes.

(*left*) Adsorption of each compound is Eads(mol) = E(surface-dimer) - E(NA) - E(NFA) -E(surface) = -0.27 eV, adsorption of the dimer is Eads(dimer) = E(surface-dimer) - E(dimer) -E(surface) = -0.17 eV, adsorption of NFA on preadsorbed NA, is

Eads(NFA/NA) = E(surface-dimer) - E(surface-NA) - E(NFA) -E(surface) = -1.13 eV. (*right*) Adsorption of each compound is (E_{ads}(mol)=of -1.28 eV; adsorption of the dimer is E_{ads}(dimer)=of -0.84 eV; and adsorption of NFA on preadsorbed NA is E_{ads}(NFA/NA)=-1.05 eV). A negative energy indicates an exothermic process.

Adsorption on diaspore. The same tendencies were observed in the case of diaspore, which is isomorph to goethite. Fig. S14 shows the adsorbed NFA molecule on diaspore surface. NA adsorption was studied in the outer and inner sphere modes. Adsorption of NA is exothermic by 0.34 eV in the outer-sphere with formation of an H-bond cycle between the molecule and two surface water molecules. Adsorption in the inner sphere mode is endothermic by 0.44 eV.

A)	B)
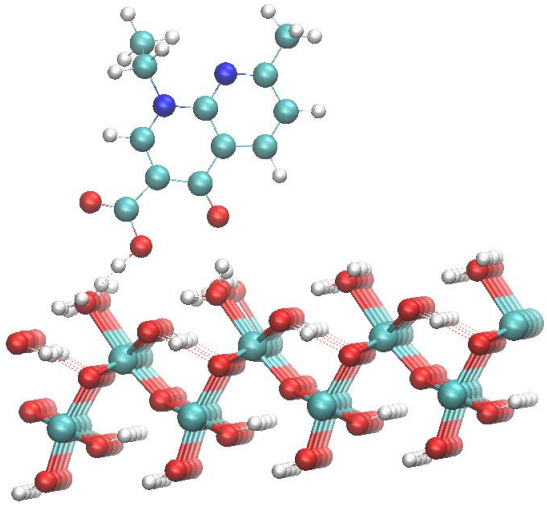	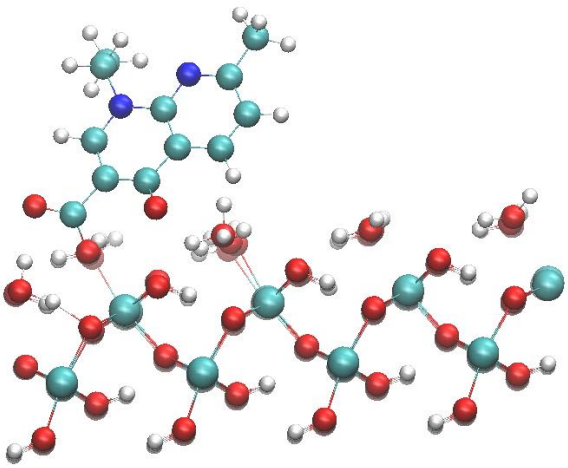
Eads(NA) = -0.34 eV	Eads(NA) = +0.44

Figure S14. A) Outer and B) inner sphere adsorption of NA on diaspore (010).

Fig.S15 shows the adsorbed NFA molecule on diaspore surface.

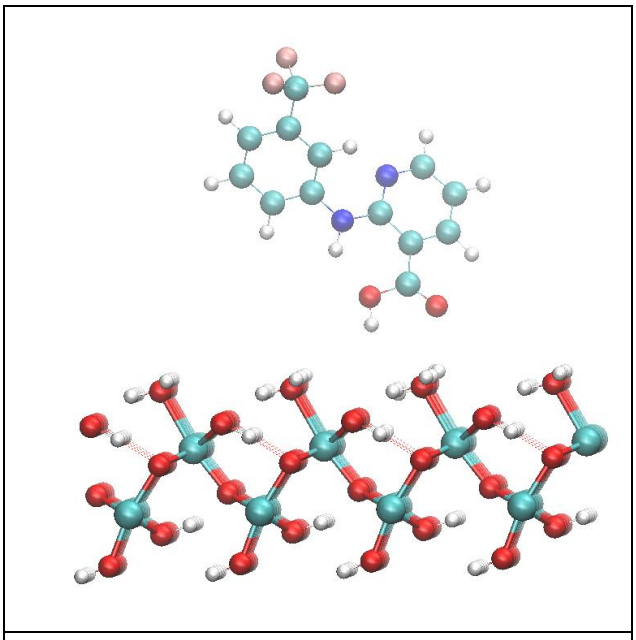

Figure S15. Adsorption of NFA on diaspore (010) ; Eads(NFA) = 0.03 eV

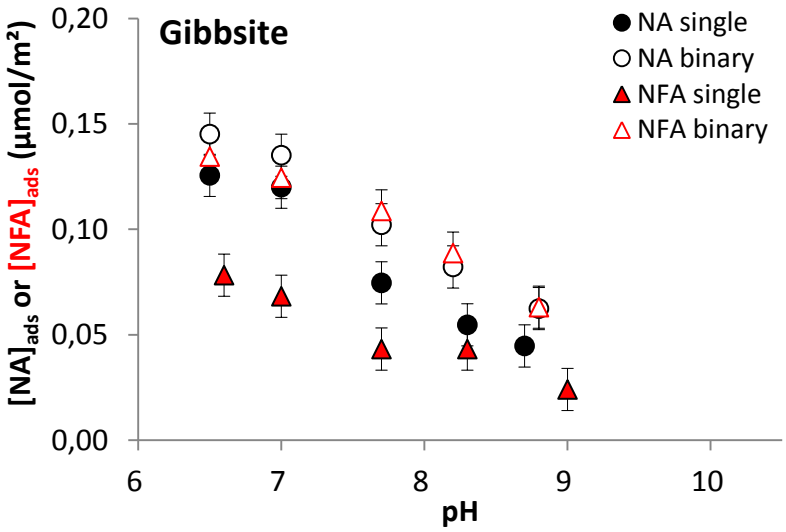

Figure S16. pH-adsorption edges of NA ($[NA]_{tot}$ = 20 µM) and NFA($[NFA]_{tot}$ = 20 µM) with 10 mM NaCl in single and binary systems on 1 g/L gibbsite.

Gibbsite ($Al(OH)_3$) was synthesized as described elsewhere in ref. 20.

IX. References

(1) Mazeina, L.; Navrotsky, A. Surface Enthalpy of Goethite. *Clays Clay Miner.* **2005**, *53* (2), 113–122.

(2) Jodin, M. C.; Gaboriaud, F.; Humbert, B. Limitations of potentiometric studies to determine the surface charge of gibbsite γ-Al(OH)3 particles. *J. Colloid Interface Sci.* **2005**, *287* (2), 581–591.

(3) Marsac, R.; Martin, S.; Boily, J.-F.; Hanna, K. Oxolinic acid binding at goethite and akaganéite surfaces: implications for aquaculture-induced pollution. *Environ. Sci. Technol.* **2016**, *50* (2), 660–668.

(4) Ross, D. L.; Riley, C. M. Aqueous solubilities of some variously substituted quinolone antimicrobials. *Int. J. Pharm.* **1990**, *63* (3), 237–250.

(5) Pobudkowska, A.; Domańska, U. Study of pH-dependent drugs solubility in water. *Chem. Ind. Chem. Eng. Q.* **2014**, *20* (1), 115–126.

(6) Takács-Novák, K.; Tam, K. Y. Multiwavelength spectrophotometric determination of acid dissociation constants: Part V: microconstants and tautomeric ratios of diprotic amphoteric drugs. *J. Pharm. Biomed. Anal.* **2000**, *21* (6), 1171–1182.

(7) Trivedi, P.; Vasudevan, D. Spectroscopic investigation of ciprofloxacin speciation at the goethite-water interface. *Environ. Sci. Technol.* **2007**, *41* (9), 3153–3158.

(8) Madey, T. E.; Yates Jr, J. T. *Vibrational spectroscopy of molecules on surfaces*; Springer Science & Business Media, 2013; Vol. 1.

(9) Nakamoto, K. *Infrared and Raman Spectra of Inorganic and Coordination Compounds. Part B: Applications in Coordination, Organometallic, and Biorganic Chemistry, 5th ed*; Wiley-Interscience: New York, 1997.

(10) Neugebauer, U.; Szeghalmi, A.; Schmitt, M.; Kiefer, W.; Popp, J.; Holzgrabe, U. Vibrational spectroscopic characterization of fluoroquinolones. *Spectrochim. Acta Part A Mol. Biomol. Spectrosc.* **2005**, *61* (7), 1505–1517.

(11) Paul, T.; Liu, J.; Machesky, M. L.; Strathmann, T. J. Adsorption of zwitterionic fluoroquinolone antibacterials to goethite: A charge distribution-multisite complexation model. *J. Colloid Interface Sci.* **2014**, *428*, 63–72.

(12) Gu, X.; Tan, Y.; Tong, F.; Gu, C. Surface complexation modeling of coadsorption of antibiotic ciprofloxacin and Cu (II) and onto goethite surfaces. *Chem. Eng. J.* **2015**, *269*, 113–120.

(13) Norén, K.; Persson, P. Adsorption of monocarboxylates at the water/goethite interface: The importance of hydrogen bonding. *Geochim. Cosmochim. Acta* **2007**, *71* (23), 5717–5730.

(14) Akyuz, S.; Akyuz, T. FT-IR spectroscopic investigations of adsorption of 2-, 3-and 4-pyridinecarboxamide on montmorillonite and saponite from Anatolia. *Vib. Spectrosc.* **2006**, *42* (2), 387–391.

(15) Balci, K.; Akkaya, Y.; Akyuz, S. An experimental and theoretical vibrational spectroscopic study on niflumic acid, a non-steroidal anti-inflammatory drug. *Vib. Spectrosc.* **2010**, *53* (2), 239–247.

(16) Saalfeld, H.; Wedde, M. Refinement of the crystal structure of gibbsite,

Al(OH)3. *Zeitschrift für Krist. Mater.* **1974**, *139* (1–6), 129–135.

(17) Gan, Y.; Franks, G. V. Charging Behavior of the Gibbsite Basal (001) Surface in NaCl Solution Investigated by AFM Colloidal Probe Technique. *Langmuir* **2006**, *22* (14), 6087–6092.

(18) Pawley, A. R.; Redfern, S. A. T.; Holland, T. J. B. Volume behavior of hydrous minerals at high pressure and temperature: I. Thermal expansion of lawsonite, zoisite, clinozoisite, and diaspore. *Am. Mineral.* **1996**, *81* (3–4), 335–340.

(19) Kubicki, J. D.; Paul, K. W.; Sparks, D. L. Periodic density functional theory calculations of bulk and the (010) surface of goethite. *Geochem. Trans.* **2008**, *9* (1), 4.

(20) Jodin, M. C.; Gaboriaud, F.; Humbert, B. Limitations of potentiometric studies to determine the surface charge of gibbsite γ-$Al(OH)_3$ particles. *J. Colloid Interface Sci.* **2005**, *287* (2), 581–591.